PHYSICAL REVIEW C, VOLUME 63, 021306(R)

Critical temperature for quenching of pair correlations

A. Schiller, A. Bjerve, M. Guttormsen, M. Hjorth-Jensen, F. Ingebretsen, E. Melby, S. Messelt, J. Rekstad, S. Siem, and S. W. Ødegård

Department of Physics, University of Oslo, P.O. Box 1048, Blindern, N-0316 Oslo, Norway

(Received 4 October 2000; published 22 January 2001)

The level density at low spin in the ^{161,162}Dy and ^{171,172}Yb nuclei has been extracted from primary γ rays. The nuclear heat capacity is deduced within the framework of the canonical ensemble. The heat capacity exhibits an S-formed shape as a function of temperature, which is interpreted as a fingerprint of the phase transition from a strongly correlated to an uncorrelated phase. The critical temperature for the quenching of pair correlations is found at $T_c = 0.50 \pm 0.04\,(\mathrm{stat}) \pm 0.08(\mathrm{syst})$ MeV.

DOI: 10.1103/PhysRevC.63.021306 PACS number(s): 21.10.Ma, 24.10.Pa, 25.55.Hp, 27.70.+q

The thermodynamical properties of nuclei deviate from infinite systems. While the quenching of pairing in superconductors is well described as a function of temperature, the nucleus represents a finite many-body system characterized by large fluctuations in the thermodynamic observables. A long-standing problem in experimental nuclear physics has been to observe the transition from strongly paired states, at zero temperature, to unpaired states at higher temperatures.

In nuclear theory, the pairing gap parameter Δ can be studied as a function of temperature using the BCS gap equations [1,2]. From this model the gap decreases monotonically to zero at a critical temperature of $T_c \sim 0.5\Delta$. However, if the particle number is projected out [3,4], the decrease is significantly delayed. The predicted decrease of pair correlations takes place over several MeV of excitation energy [4]. Recently [5], we reported fine structures in the level densities in the 1–7 MeV region, which are probably due to the breaking of individual nucleon pairs and a gradual decrease of pair correlations.

Experimental data on the quenching of pair correlations are important as a test for nuclear theories. Within finite temperature BCS and RPA models, level density and specific heat are calculated for, e.g., ^{58}Ni [6]; within the shell model Monte Carlo (SMMC) method [7,8] one is now able to estimate level densities [9,10] in heavy nuclei [11] up to high excitation energies. Level density and specific heat for several heavy and deformed nuclei have also been calculated within the finite temperature Hartree-Fock-Bogoliubov method [12].

The subject of this Rapid Communication is to report on the observation of the gradual transition from strongly paired states to unpaired states in rare earth nuclei at low spin. The canonical heat capacity is used as a thermometer. Since only particles at the Fermi surface contribute to this quantity, it is very sensitive to phase transitions. It has been demonstrated from SMMC calculations in the Fe region [13–15] that breaking of only one nucleon pair increases the heat capacity significantly.

Recently [16,17], we presented a method for extracting level density and γ-ray strength function from measured γ-ray spectra. Since the γ-decay half-lives are long, typically 10^{-12}–10^{-19} s, the method should essentially give observables from a thermalized system [18]. The spin window is typically 2–6 $\hbar$ and the excitation energy resolution is 0.3 MeV.

The experiments were carried out with 45 MeV ^{3}He projectiles from the MC-35 cyclotron at the University of Oslo. The experimental data were recorded with the CACTUS multidetector array [19] using the $(^3\mathrm{He},\alpha\gamma)$ reaction on ^{162,163}Dy and ^{172,173}Yb self-supporting targets. The beam time was two weeks for each target. The charged ejectiles were detected with eight particle telescopes placed at an angle of 45° relative to the beam direction. Each telescope comprises one Si ΔE front and one Si(Li) E end detector with thicknesses of 140 and 3000 μm, respectively. An array of 28 5 in.$\times$5 in. NaI(Tl) γ detectors with a total efficiency of $\sim$15% surrounded the target and particle detectors.

From the reaction kinematics the measured α-particle energy can be transformed to excitation energy E. Thus, each coincident γ ray can be assigned a γ cascade originating from a specific excitation energy. The data are sorted into a matrix of (E,E_γ) energy pairs. At each excitation energy E the NaI γ-ray spectra are unfolded [20], and this matrix is used to extract the primary γ-ray matrix, with the well established subtraction technique of Ref. [21].

The resulting matrix $P(E,E_\gamma)$, which describes the primary γ-ray spectra obtained at an initial excitation energy E, is factorized according to the Brink-Axel hypothesis [22,23] by $P(E,E_\gamma) \propto \rho(E-E_\gamma)F(E_\gamma)$. The level density $\rho(E)$ and the γ-ray energy-dependent factor $F(E_\gamma)$ are determined by a least χ^2 fit to P. Since the fit yields an infinitely large number of equally good solutions, which can be obtained by transforming one arbitrary solution by [17]

$$\tilde{\rho}(E-E_\gamma) = A\exp[\alpha(E-E_\gamma)]\rho(E-E_\gamma), \tag{1}$$

$$\tilde{F}(E_\gamma) = B\exp(\alpha E_\gamma)F(E_\gamma), \tag{2}$$

we have to determine the parameters A, B, and α by comparing the ρ and F functions to known data. The A and α parameters are fitted to reproduce the number of known levels in the vicinity of the ground state [24] and the neutron resonance spacing at the neutron binding energy [25].

Figure 1 shows the extracted level densities and γ-ray energy-dependent factors for the ^{161,162}Dy and ^{171,172}Yb nuclei. The data are identical to those in [26], where the γ-ray strength function is discussed thoroughly.

The partition function in the canonical ensemble

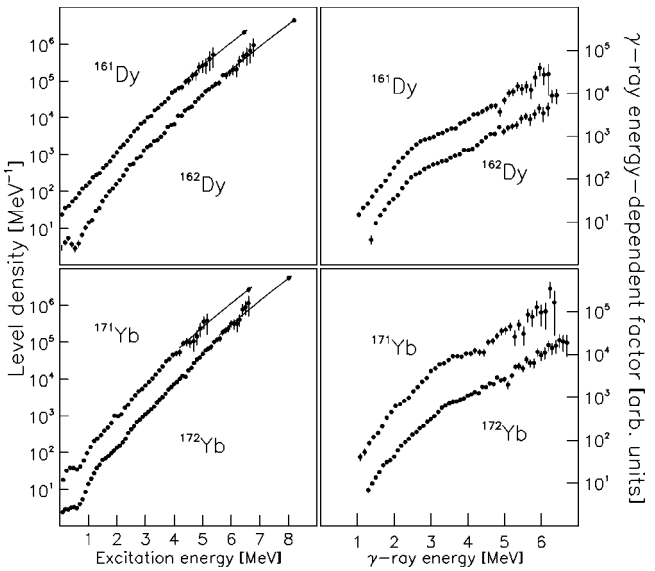

FIG. 1. Experimental level density (points in left panels) and γ-ray energy-dependent factor (right panels) for ^{161,162}Dy (upper part) and ^{171,172}Yb (lower part). The error bars show the statistical uncertainties. The solid lines are extrapolations based on a shifted Fermi gas model (see text). The isolated point at the neutron binding energy is obtained from neutron resonance spacing data.

$$Z(T)=\sum_{n=0}^{\infty}\rho(E_n)e^{-E_n/T} \tag{3}$$

is determined by the measured level density of accessible states $\rho(E_n)$ in the present nuclear reaction. Strictly, the sum should run from zero to infinity. In this work we calculate Z for temperatures up to $T=1$ MeV. Assuming a Bethe-like level density expression [27], the average excitation energy in the canonical ensemble

$$\langle E(T)\rangle=Z^{-1}\sum_{n=0}^{\infty}E_n\rho(E_n)e^{-E_n/T} \tag{4}$$

gives roughly $\langle E\rangle\sim aT^2$ with a standard deviation of $\sigma_E\sim T\sqrt{2aT}$ where a is the level density parameter. Using Eq. (4) requires that the level density should be known up to $\langle E\rangle+3\sigma_E$, typically 40 MeV. However, the experimental level densities of Fig. 1 only cover the excitation region up close to the neutron binding energy of about 6 and 8 MeV for odd and even mass nuclei, respectively. For higher energies it is reasonable to assume Fermi gas properties, since single particles are excited into the continuum region with high level density. Therefore, due to lack of experimental data, the level density is extrapolated to higher energies by the shifted Fermi gas model expression [28]

$$\rho_{\mathrm{FG}}(U)=f\frac{\exp(2\sqrt{aU})}{12\sqrt{0.1776}a^{1/2}U^{3/2}A^{1/3}}, \tag{5}$$

where U is the shifted energy and A is the mass number. For shift and level density parameters a, we use the parametrization of von Egidy *et al.* [29]. The expression had to be normalized by a factor f in order to match the neutron resonance spacing data. The factors are 1.2, 0.9, 0.6, and 0.6 for ^{161,162}Dy and ^{171,172}Yb, respectively. The solid lines in Fig. 1 show how the expression extrapolates our experimental level density curves.

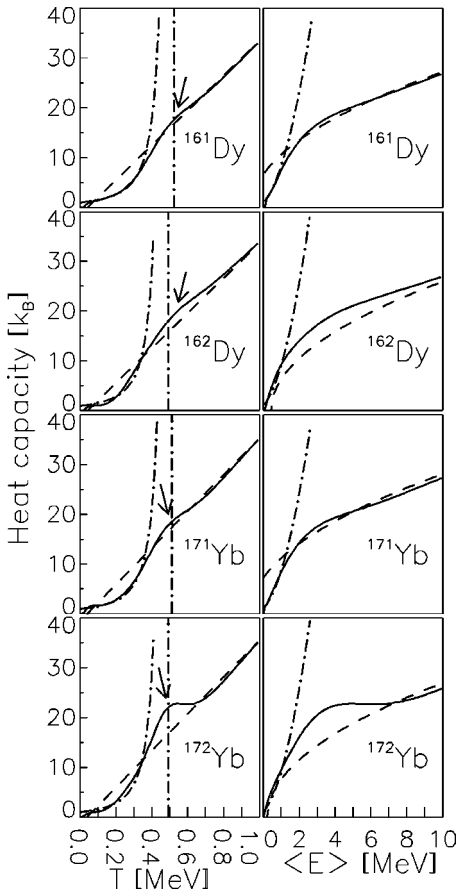

FIG. 2. Semiexperimental heat capacity as a function of temperature (left panels) and energy $\langle E\rangle$ (right panels) in the canonical ensemble for ^{161,162}Dy and ^{171,172}Yb. The dashed lines describe the approximate Fermi gas heat capacity. The arrows indicate the first local maxima of the experimental curve relative to the Fermi gas estimates. The dash-dotted lines describe estimates according to Eq. (9) where τ is set equal to the critical temperature T_c. T_c is indicated by the vertical lines.

The extraction of the microcanonical heat capacity $C_V(E)$ gives large fluctuations which are difficult to interpret [5]. Therefore, the heat capacity $C_V(T)$ is calculated within the canonical ensemble, where T remains fixed and is the more appropriate parameter. The heat capacity is then given by

$$C_V(T)=\frac{\partial\langle E\rangle}{\partial T}, \tag{6}$$

and the averaging made in Eq. (4) gives a smooth temperature dependence of $C_V(T)$. A corresponding $C_V(\langle E\rangle)$ may also be derived in the canonical ensemble.

The deduced heat capacities for the ^{161,162}Dy and ^{171,172}Yb nuclei are shown in Fig. 2. All four nuclei exhibit similarly S-shaped $C_V(T)$-curves with a local maximum relative to the Fermi gas estimate at $T_c\approx 0.5$ MeV. The

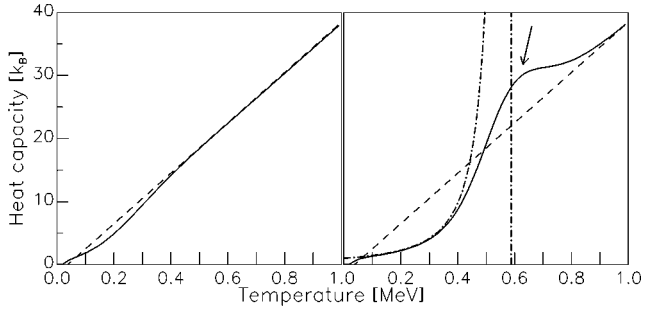

FIG. 3. A pure Fermi gas model cannot give rise to the characteristic S shape of the canonical heat capacity curve $C_V(T)$ (left panel). A simple composite level density can schematically simulate our experimental findings (right panel).

S-shaped curve is interpreted as a fingerprint of a phase transition in a finite system from a phase with strong pairing correlations to a phase with weak pairing correlations described in very recent theoretical calculations [12,15]. Due to the strong smoothing introduced by the transformation to the canonical ensemble, we do not expect to see discrete transitions between the various quasiparticle regimes as we do in Ref. [5], but only the transition where all pairing correlations are quenched as a whole. In the right panels of Fig. 2, we see that $C_V(\langle E\rangle)$ strongly increases in the first MeV of excitation energy. The shape of this structure confirms the expectation that the pair correlations are quenched over a wide excitation energy region [5].

In the following, we will extract the critical temperature for the quenching of pairing correlations from our data. An inspection of Fig. 1 shows that the level density is roughly composed of two components as proposed by Gilbert and Cameron [28]: (i) a low energetic part; approximately a straight line in the log plot, and (ii) a high energetic part including the theoretical Fermi gas extrapolation; a slower growing function. In order to model the observed behavior of the $C_V(T)$ curves on Fig. 2, we construct a simple level density formula composed of a constant temperature level density part with τ as temperature parameter, and a Fermi gas expression

$$\rho(E)\propto\begin{cases}\eta\exp(E/\tau) & \text{for } E\leqslant\varepsilon\\ E^{-3/2}\exp(2\sqrt{aE}) & \text{for } E>\varepsilon,\end{cases}\tag{7}$$

where $\eta=\varepsilon^{-3/2}\exp(2\sqrt{a\varepsilon}-\varepsilon/\tau)$ accounts for continuity at the energy $E=\varepsilon$. If we also require the slopes to be equal at ε, the level density parameter a is restricted to

$$a=\left(\frac{\sqrt{\varepsilon}}{\tau}+\frac{3}{2\sqrt{\varepsilon}}\right)^2.\tag{8}$$

Figure 3 shows the heat capacity evaluated in the canonical ensemble with the level density function of Eq. (7) and $\tau^{-1}=1.7\ \text{MeV}^{-1}$. The left-hand part simulates a pure Fermi gas description, i.e., the case $\varepsilon=0$, assuming a level density parameter $a=20\ \text{MeV}^{-1}$. One can see that a pure Fermi gas does not give rise to the characteristic S shape of the heat capacity. The right-hand part simulates the experiments,

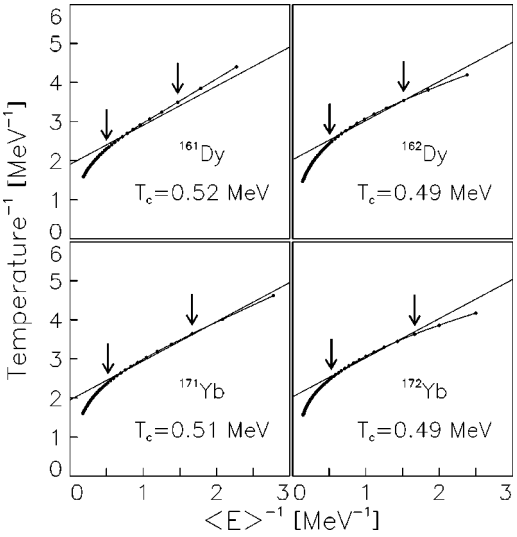

FIG. 4. The critical temperature is deduced by fitting a straight line with slope 1 to the data points between the arrows.

where $\varepsilon=5$ MeV and a fulfills Eq. (8), i.e., again $a=20\ \text{MeV}^{-1}$. The characteristic S-shape emerges, as also seen in the experimental data of Fig. 2.

Therefore, our method to find T_c relies on the assumption that the lower energetic part of the level density can be approximately described by a constant temperature level density. Calculating $\langle E(T)\rangle$ and $C_V(T)$ within the canonical ensemble for a purely exponential level density gives $T^{-1}=\langle E(T)\rangle^{-1}+\tau^{-1}$ and

$$C_V(T)=(1-T/\tau)^{-2}.\tag{9}$$

Thus, plotting T^{-1} as function of $\langle E(T)\rangle^{-1}$ one can determine τ from Fig. 4. The quantity τ is then identified with the critical temperature T_c, since $C_V(T)$ according to Eq. (9) exhibits a pole at τ and the analogy with the definition of T_λ in the theory of superfluids becomes evident. The $C_V(T)$ curve of Eq. (9) with $T_c=\tau$ using the extracted critical temperatures for the four nuclei is shown as dash-dotted lines in Fig. 2. This simple analytical expression with only one parameter T_c describes well the experimental data up to temperatures of $\sim$0.4 MeV. The critical temperature itself is marked by the vertical lines. The extracted T_c is rather close to the other estimate of T_c represented by the arrows. The extracted values are $T_c=0.52$, 0.49, 0.51, and 0.49 MeV for the ^{161,162}Dy and ^{171,172}Yb nuclei, respectively, which are somehow delayed compared to a degenerated BCS model with $T_c=0.5\Delta$ yielding $T_c\sim0.44$, 0.46, 0.37, and 0.40 MeV for the respective nuclei, where Δ is calculated from nucleon separation energies [24].

We will now discuss how sensitive the extracted critical temperature is with respect to the extrapolation, and we will give an estimate of the uncertainty of the extracted critical temperatures. In the fit in Fig. 4, we use only energies from $\langle E\rangle\sim0.5$–2 MeV. This corresponds to energies in the level density curves up to $E_n\sim6$ MeV according to Eq. (4). Also, in Fig. 2, the interval where Eq. (9) describes the experimental data is $T\sim0$–0.4 MeV. This corresponds to energies in

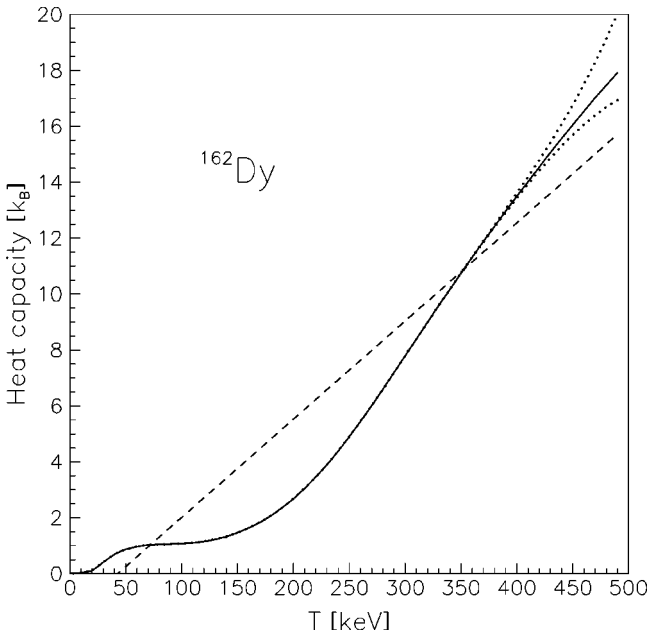

FIG. 5. Canonical $C_V(T)$ curves of ^{162}Dy derived with different extrapolations of the experimental level density curve above B_n. The extrapolations are performed at the extremes (dotted lines) of the parametrization of von Egidy *et al.* [29], i.e., at $a=12.9$ and 23.4 MeV^{-1} and $C_1=-0.5$ and -2.7 MeV and multiplied with a factor f such that they agree with the level density at B_n derived from neutron resonance spacing. The solid and dashed lines are equal to those in Fig. 2. The heat capacity curve below $T\sim0.4$ MeV is not affected by the different extrapolations. The dotted lines can be regarded as typical error bands for all four nuclei.

the level density curves up to $E_n\sim8$ MeV. Thus, the extracted critical temperature from the low-energy behavior of the $T(\langle E\rangle)$ and $C_V(T)$ curves does only depend weakly on the actual extrapolation of the energy dependence of the ρ curve. Also, the S shape of the $C_V(T)$ curve depends only on the fact that the nuclear level density develops somehow as a Fermi gas expression at energies somewhere above the neutron binding energy (see Fig. 5). The main contribution to the statistical error in the critical temperature comes from the uncertainty of the slope of the experimental level density curve. Since this slope is well determined by the counting of discrete levels on one end and the neutron resonance spacing data on the other end, we estimate the statistical error of T_c being ~0.04 MeV. It is also important to notice, that due to the strong smoothing in Eq. (4), the errors of the experimental level density curves are negligible in our calculation. However, one should keep in mind that, by our method, critical temperatures of the order 0.5 MeV are determined from the shapes of the $T(\langle E\rangle)$ and $C_V(T)$ curves up to only $T\sim0.35$ MeV. Certainly a systematic error will be introduced due to this extrapolation, since Figs. 2 and 4 show that the simple functional form of Eq. (9) does not describe the data above $T\sim0.4$ MeV. Anyway, the actual values of the $C_V(T)$ curves above $T\sim0.4$ MeV depend on the specific extrapolation of the experimental level density curves. We estimate roughly the systematic error of T_c introduced by the extrapolation being 0.08 MeV.

In conclusion, we have seen a fingerprint of a phase transition in a finite system for the quenching of pairing correlations as a whole, given by the S shape of the canonical heat capacity curves in rare earth nuclei. For the first time the critical temperature T_c at which pair correlations in rare earth nuclei are quenched, has been extracted from experimental data. The observed S shape of the heat capacity agrees well with recent theoretical findings.

The authors are grateful to E.A. Olsen and J. Wikne for providing the excellent experimental conditions. We thank Y. Alhassid for several interesting discussions. We wish to acknowledge the support from the Norwegian Research Council (NFR).

[1] M. Sano and S. Yamasaki, Prog. Theor. Phys. **29**, 397 (1963).
[2] A. L. Goodman, Nucl. Phys. **A352**, 45 (1981).
[3] A. Faessler, K. R. Sandhya Devi, F. Grümmer, K. W. Schmid, and R. R. Hilton, Nucl. Phys. **A256**, 106 (1976).
[4] T. Døssing *et al.*, Phys. Rev. Lett. **75**, 1276 (1995).
[5] E. Melby, L. Bergholt, M. Guttormsen, M. Hjorth-Jensen, F. Ingebretsen, S. Messelt, J. Rekstad, A. Schiller, S. Siem, and S. W. Ødegård, Phys. Rev. Lett. **83**, 3150 (1999).
[6] Nguyen Dinh Dang, Z. Phys. A **335**, 253 (1990).
[7] G. H. Lang, C. W. Johnson, S. E. Koonin, and W. E. Ormand, Phys. Rev. C **48**, 1518 (1993).
[8] S. E. Koonin, D. J. Dean, and K. Langanke, Phys. Rep. **278**, 1 (1997).
[9] H. Nakada and Y. Alhassid, Phys. Rev. Lett. **79**, 2939 (1997).
[10] W. E. Ormand, Phys. Rev. C **56**, R1678 (1997).
[11] J. A. White, S. E. Koonin, and D. J. Dean, Phys. Rev. C **61**, 034303 (2000).
[12] J. L. Egido, L. M. Robledo, and V. Martin, Phys. Rev. Lett. **85**, 26 (2000).
[13] S. Rombouts, K. Heyde, and N. Jachowicz, Phys. Rev. C **58**, 3295 (1998).
[14] Y. Alhassid, S. Liu, and H. Nakada, Phys. Rev. Lett. **83**, 4265 (1999).
[15] S. Liu and Y. Alhassid, nucl-th/0009006.
[16] L. Henden, L. Bergholt, M. Guttormsen, J. Rekstad, and T. S. Tveter, Nucl. Phys. **A589**, 249 (1995).
[17] A. Schiller, L. Bergholt, M. Guttormsen, E. Melby, J. Rekstad, and S. Siem, Nucl. Instrum. Methods Phys. Res. A **447**, 498 (2000).
[18] A. Schiller, M. Guttormsen, E. Melby, J. Rekstad, and S. Siem, Phys. Rev. C **61**, 044324 (2000).
[19] M. Guttormsen, A. Atac, G. Løvhøiden, S. Messelt, T. Ramsøy, J. Rekstad, T. F. Thorsteinsen, T. S. Tveter, and Z. Zelazny, Phys. Scr. **T32**, 54 (1990).
[20] M. Guttormsen, T. S. Tveter, L. Bergholt, F. Ingebretsen, and J. Rekstad, Nucl. Instrum. Methods Phys. Res. A **374**, 371 (1996).

[21] M. Guttormsen, T. Ramsøy, and J. Rekstad, Nucl. Instrum. Methods Phys. Res. A **255**, 518 (1987).
[22] D. M. Brink, Ph.D. thesis, Oxford University, 1955.
[23] P. Axel, Phys. Rev. **126**, 671 (1962).
[24] R. B. Firestone and V. S. Shirley, *Table of Isotopes*, 8th ed. (Wiley, New York, 1996), Vol. II.
[25] A. S. Iljinov, M. V. Mebel, N. Bianchi, E. De Sanctis, C. Guaraldo, V. Lucherini, V. Muccifora, E. Polli, A. R. Reolon, and P. Rossi, Nucl. Phys. **A543**, 517 (1992).
[26] A. Voinov, M. Guttormsen, E. Melby, J. Rekstad, A. Schiller, and S. Siem, nucl-ex/0009018.
[27] H. A. Bethe, Phys. Rev. **50**, 332 (1936).
[28] A. Gilbert and A. G. W. Cameron, Can. J. Phys. **43**, 1446 (1965).
[29] T. von Egidy, H. H. Schmidt, and A. N. Behkami, Nucl. Phys. **A481**, 189 (1987), Eq. (10).